Journal of Alloys and Compounds 509 (2011) 3672–3676

Contents lists available at ScienceDirect

Journal of Alloys and Compounds

journal homepage: www.elsevier.com/locate/jallcom

A study of structural, optical and magnetic properties of $Zn_{0.97-x}Cu_xCr_{0.03}O$ diluted magnetic semiconductors

Jinghai Yang[a,b,c,*], Lianhua Fei[a,b], Huilian Liu[a,b], Yang Liu[a,b], Ming Gao[a,b], Yongjun Zhang[a,b], Lili Yang[a,b]

[a] Institute of Condensed State Physics, Jilin Normal University, Siping 136000, People's Republic of China
[b] Key Laboratory of Functional Materials Physics and Chemistry, Jilin Normal University, Ministry of Education, Siping 136000, People's Republic of China
[c] National Laboratory of Superhard Materials, Jilin University, Changchun 130012, People's Republic of China

ARTICLE INFO

Article history:
Received 23 August 2010
Received in revised form
21 December 2010
Accepted 21 December 2010
Available online 28 December 2010

Keywords:
Diluted magnetic semiconductors
ZnO samples
Cr
Cu co-doping
Ferromagnetism

ABSTRACT

A set of $Zn_{0.97-x}Cu_xCr_{0.03}O$ ($0 \le x \le 0.03$) samples has been synthesized by the sol–gel method. The structural, optical and magnetic properties of the samples were investigated by X-ray diffraction (XRD), X-ray photoelectron spectroscopy (XPS), photoluminescence (PL) and vibrating sample magnetometer (VSM). With Cu doping concentration increasing up to 2 at%, the XRD results showed that all diffraction peaks corresponded to wurtzite structure of ZnO, but for $Zn_{0.94}Cu_{0.03}Cr_{0.03}O$, the secondary phase of Cu emerged. PL measurements showed that $Zn_{0.97-x}Cu_xCr_{0.03}O$ powders and pure ZnO with the Cu concentration varied from 0.00 to 0.02 exhibited obvious blue shift; the green emission peak could be effectively enhanced with the increase of the Cu concentration. Magnetic measurements indicated that room-temperature ferromagnetism of $Zn_{0.97-x}Cu_xCr_{0.03}O$ was an intrinsic property when Cu concentration was less than 0.02. The saturation magnetization of $Zn_{0.97-x}Cu_xCr_{0.03}O$ ($x = 0$, 0.01, 0.02) increased with the increase of the Cu concentration.

1. Introduction

Oxide-diluted magnetic semiconductors (O-DMSs) based on ZnO, TiO_2 and SnO_2 have attracted great attention in recent years due to the possibility of inducing room temperature ferromagnetism. Since ZnO has a wide bandgap energy ($E_g = 3.37$ eV) and is a promising transparent ferromagnetic material, ZnO DMS has been intensively studied for its advanced spintronic application in recent years [1]. A theoretical prediction pointed out that room-temperature (RT) ferromagnetism (FM) can be obtained in p-type Mn-doped ZnO [2]. In succession, further theoretical calculation has been carried on the ZnO doped with Cr, V, Fe, Ni and Co and predicted that they should exhibit ferromagnetic properties [3]. Both experimental results and theoretical calculations revealed that different transition metal ions and carrier concentration in the ZnO based DMSs would strongly influence their properties [4–14].

Recently, many researchers have tried to dope other ions into the ZnO based DMSs to obtain two metal ions co-doped ZnO in order to change their optical and magnetic properties by introducing additional carriers [15–19]. Lin et al. supposed that a small amount of additional Cu doping would create additional carriers in Co doping ZnO, and its magnetization would be greatly enhanced in bulk samples [20]. N. Brihi et al. asserted that the anti-ferromagnetism of $Zn_{0.97}Mn_{0.03}O$ polycrystalline increased after Al-doping [21]. Lu et al. also declared that compared with weak ferromagnetism in the Co-doped ZnO single crystalline film, the film with additional Al co-doping had much stronger ferromagnetic order at room temperature [4].

So far, according to the Cr-doped ZnO, we cannot determine that the ferromagnetic order actually arises from the Cr ion substitution in the lattice or the secondary phases [22]. Another thing to be revealed is the effect of donor and acceptor impurity bands on the magnetic couplings [23–25]. Therefore, we chose Cr and Cu as doping elements, because unlike many other metals, Cr itself is anti-ferromagnetic and an extrinsic ferromagnetism cannot be induced even if Cr clustering occurs [26]. In addition, Cu is a preferred choice to avoid controversies since the secondary phases such as CuO, Cu_2O or Cu clusters are non-ferromagnetic, which may make the interpretation of ferromagnetism in ZnCuO easier [2,27,28].

In our previous work, we have investigated the effect of Cr-doping and Cu-doping on the optical and magnetic properties in ZnO samples [22,26]. In this work, we reported the room temperature magnetic and optical properties of $Zn_{0.97-x}Cu_xCr_{0.03}O$

* Corresponding author at: Institute of Condensed State Physics, Jilin Normal University, No. 1301, Haifeng Street, Siping, People's Republic of China.
Tel.: +86 434 3294566; fax: +86 434 3294566.
E-mail address: jhyang1@jlnu.edu.cn (J. Yang).

0925-8388/$ – see front matter © 2010 Elsevier B.V. All rights reserved.
doi:10.1016/j.jallcom.2010.12.157

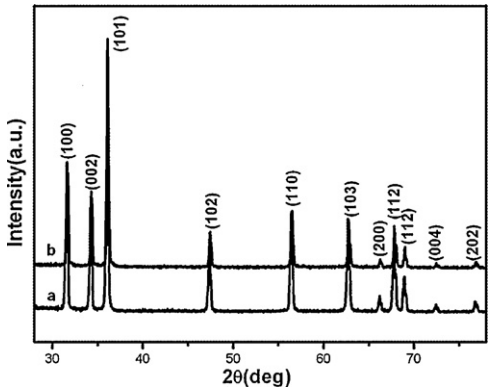

Fig. 1. XRD patterns of the pure ZnO (a) and $Zn_{0.97}Cr_{0.03}O$ (b).

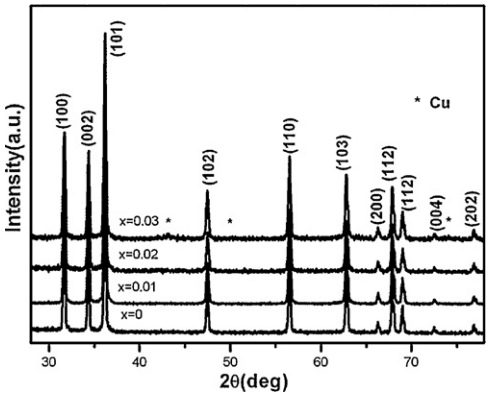

Fig. 2. XRD patterns of the $Zn_{0.97-x}Cu_xCr_{0.03}O$ ($x = 0$, 0.01, 0.02, 0.03).

($0 \le x \le 0.03$) powders prepared by the sol–gel method. This sol–gel method allows the mixing of the chemicals at the atomic level, thus the possibility of forming an undetectable impurity phase could be reduced. Hence, the physical properties of the samples prepared by this method usually exhibit their intrinsic nature. The sol–gel method also has other advantages such as good reproducibility and a simple experimental procedure [29,30]. The effect of Cu on the structure, optical and magnetic properties of ZnCrO has been studied in detail.

2. Experimental details

Appropriate proportions of Zn nitrate [$Zn(NO_3)_2{\cdot}6H_2O$] (99.9%), Cr nitrate [$Cr(NO_3)_3{\cdot}9H_2O$] (99.9%) and Cu nitrate [$Cu(NO_3)_2{\cdot}3H_2O$] (99.9%) were dissolved into citrate ($C_6H_8O_7{\cdot}H_2O$) (99.5%) aqueous solution with stirring to form the sol. Then, the mixture was polymerized to form a gel at 80 °C. After the swelled gel was pyrolyzed at 130 °C, a reticular substance was obtained, which was then grinded to powder in agate mortar. The powder was sintered at 700 °C under argon atmosphere for 10 h.

The structural characterization of Cu, Cr doped ZnO samples were performed on a D/max-2500 copper rotating-anode X-ray diffractometer with Cu Kα radiation (40 kV, 200 mA). The chemical composition of $Zn_{0.97}Cr_{0.03}O$ and $Zn_{0.95}Cu_{0.02}Cr_{0.03}O$ was determined by X-ray photoelectron spectroscopy (XPS) (VG ESCALAB Mark II). PL measurements of the samples were performed on an HR800 Labram Infinity Spectrophotometer, which was excited by a continuous He–Cd laser at a wavelength of 325 nm and a power of 10 mW. Magnetic hysteresis loops of $Zn_{0.97-x}Cu_xCr_{0.03}O$ were measured by a Lake Shore 7407 vibrating sample magnetometer.

3. Results and discussion

3.1. Structural characteristics

The XRD patterns of as-synthesized ZnO samples without and with Cr ions doping are shown in Fig. 1. There are no other impurity phases in both diffraction patterns and all diffraction peaks could be indexed to wurtzite hexagonal ZnO (space group $P63mc$). The cell constant of pure ZnO is estimated to be $a = 0.325775$ nm, $c = 0.521853$ nm, and the volume is 0.04791 nm^3 (Fig. 1a). However, the cell constant of $Zn_{0.97}Cr_{0.03}O$ is estimated to be $a = 0.325444$ nm, $c = 0.521216$ nm, and the volume is 0.04782 nm^3 (Fig. 1b), which is smaller than that of pure ZnO. The result can be ascribed to the substitution of Cr^{3+} ions with a smaller ionic radius of 0.063 nm for Zn^{2+} (0.074 nm) sites [26]. Fig. 2 shows XRD patterns for $Zn_{0.97-x}Cu_xCr_{0.03}O$ ($x = 0$, 0.01, 0.02, 0.03), in which we can see that all diffraction peaks correspond to wurtzite structure ZnO with Cu doping concentration increasing up to 2 at%. No trace of copper, chromium metal, oxides, any binary zinc copper phases, binary zinc chromium phases or ternary zinc copper chromium are discovered. For $Zn_{0.97-x}Cu_xCr_{0.03}O$ ($x = 0$, 0.01, 0.02), the radius of Cu^+ ions (0.057 nm) are smaller than that of Zn^{2+} ions (0.074 nm). Once Cu ions or Cr ions or both of them replace Zn^{2+}, the bonding length of Cu–O or Cr–O will be shorter in comparison with Zn–O. Thus, the lattice constant will decrease. However, for the case of $Zn_{0.94}Cu_{0.03}Cr_{0.03}O$, the secondary phase of Cu emerged, which indicates that the Cu ions and Cr ions would not only substitute the Zn place but also exist as interstitial ions or enter into vacancies. As a whole, the atoms are rearranged and placed on the equilibrium state due to the coulomb interaction between Zn^{2+} and O^{2-}, so the lattice constants abnormally increase [27,1].

To clearly show how Cu doping concentration influences the structural properties of ZnCrO, the lattice parameters of $Zn_{0.97-x}Cu_xCr_{0.03}O$ are summarized in Table 1. The average grain sizes are estimated from the full width at half maximum (FWHM) of three main peaks by the Debye–Scherrer formula. The Cu doping ($x = 0$, 0.01, 0.02) leads to the decrease of the interplanar distance of the (0 0 2) crystal plane, which is in agreement with the shift of the (0 0 2) peak position towards high angles [31,32]. When Cu concentration increases from 0.02 to 0.03, the interplanar distance of the (0 0 2) crystal plane increases, which can be deduced from the shift of the (0 0 2) peak position towards low angles. Above results further prove Cu successfully substitutes Zn position when Cu concentration is less than 0.02 [32]. In addition, the solid solution of Cu doping ZnCrO is 0.03.

3.2. Chemistry state

The high resolution scans of Cr 2p XPS spectra are shown in Fig. 3 for the $Zn_{0.97}Cr_{0.03}O$ and $Zn_{0.95}Cu_{0.02}Cr_{0.03}O$ samples. For $Zn_{0.97}Cr_{0.03}O$, the Cr $2p_{3/2}$ peak is located in the vicinity of 576.6 eV, which is clearly different from 574.2 eV of Cr metal and 576.0 eV of Cr^{2+} [33]. After comparison, we found that this peak can be indexed to Cr^{3+} ions, whose binding energy of Cr $2p_{3/2}$ is 576.7 eV [32]. Ordinarily, the valence of Cr should be +2 if Cr is present in the sub-

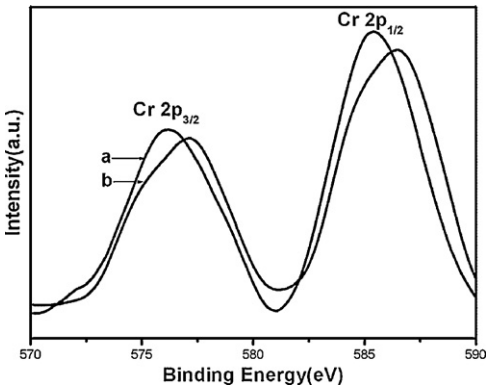

Fig. 3. The Cr 2p core-level photoemission spectra for $Zn_{0.97}Cr_{0.03}O$ (a) and $Zn_{0.95}Cr_{0.03}Cu_{0.02}O$ (b) samples at room temperature.

Table 1
Summary of cell parameters, grain size of Cu and Cr codoped ZnO.

Sample	a (nm)	c (nm)	Vol. (nm^3)	d (0 0 2) (nm)	Averaged grain size (nm)
$Zn_{0.97}Cu_{0.00}Cr_{0.03}O$	0.32544	0.52122	0.04787	0.26083	61.3
$Zn_{0.96}Cu_{0.01}Cr_{0.03}O$	0.32541	0.52121	0.04779	0.26065	54.4
$Zn_{0.95}Cu_{0.02}Cr_{0.03}O$	0.32538	0.52115	0.04778	0.26063	47.5
$Zn_{0.94}Cu_{0.03}Cr_{0.03}O$	0.32545	0.52080	0.04777	0.26084	44.0

stitutional site in a defect-free ZnO crystal. However, in our case, we can deduce that Cr dopants probably incorporate into the ZnO lattice as Cr^{3+} ions on the basis of the XPS results. As shown in Fig. 3(b), we can find that the Cr $2p_{3/2}$ peak position for $Zn_{0.95}Cu_{0.02}Cr_{0.03}O$ sample is located at 577.1 eV after fitting with the Gaussian function. The peak position is clearly different from that of Cr metal and Cr^{2+}. But it is quite close to the peak position of Cr $2p_{3/2}$ in Cr_2O_3 [15,33]. It further suggests that Cr dopants are actually incorporated into the ZnO lattice as Cr^{3+} ions [26]. That is to say, the entrance of Cu irons in ZnCrO does not change the valence state of Cr. However, the binding energy of the Cr 2p enlarges with Cu doping. According to the XRD result, with increasing Cu doping concentration, not only the lattice parameters decrease but also the distance between Cr ions becomes shorter, which will make the binding energy of Cr 2p increase. Of course, the environment of Cr coordination changing due to Cu doping was another possible reason for the increase of binding energy of Cr 2p.

The valence state of Cu for $Zn_{0.95}Cu_{0.02}Cr_{0.03}O$ is also determined by XPS spectra. As shown in Fig. 4, the peaks located at 932.4 eV and 951.6 eV can be ascribed to Cu $2p_{3/2}$ and Cu $2p_{1/2}$ peak respectively. It is expected that the Cu^+ $2p_{3/2}$ and $2p_{1/2}$ peaks would locate at 932.5 and 952.3 eV, while Cu^{2+} $2p_{3/2}$ and $2p_{1/2}$ peaks would locate at 933.7 and 953.6 eV, respectively. Therefore, we can conclude that the Cu ions present as +1 valence state [23].

3.3. Optical properties

In order to study the effect of Cu doping concentration on the optical properties of $Zn_{0.97-x}Cu_xCr_{0.03}O$ ($x = 0$, 0.01, 0.02) samples, PL spectra are shown in Fig. 5. To make the comparison clear, the PL spectrum of pure ZnO is also illustrated here. We can observe that all the spectra contain a strong UV band peak around 380 nm, which commonly originates from excitonic recombination corresponding to the near-band-edge emission of ZnO [34,35]. Compared with pure ZnO, on the one hand, for the PL spectra from $Zn_{0.97-x}Cu_xCr_{0.03}O$ ($x = 0$, 0.01, 0.02), the peak position of UV emission exhibits a blue shift with Cu doping concentration increasing to 0.02. To see it clearly, we enlarge the UV region of all the spectra in the inset of Fig. 5. On the other hand, with the increase of Cu doping concentration from 0 to 0.02, the intensity of the green emission band is enhanced, and especially sharply increases when Cu concentration increases from 0.01 to 0.02. The near-band-edge emission is a process related to the crystal volume. A decrease of crystal size not only causes a blue shift in the emission wavelength due to the confinement effect, but also leads to a change in the energy transfer from excited states to the ground state [36]. The green emission peak is commonly referred as deep-level or trap-state emission [37,38]. Various mechanisms have been proposed for the green emission of ZnO [39]. Oxygen vacancy was recently testified to be one of the origins of green emission in ZnO, which occurs in three different charge states: the neutral oxygen vacancy (Vo), the singly ionized oxygen vacancy ($Vo^{\bullet}$), and the doubly ionized oxygen vacancy ($Vo^{\bullet\bullet}$) [40]. In comparison with the PL spectra of ZnCrO, it can be observed that Cu doping could effectively enhance the green emission in the $Zn_{0.97-x}Cu_xCr_{0.03}O$ (0.01, 0.02) powders. The enhanced intensity of the green emission indicates that the density of defects increases, which could be attributed to Cu doping since Cu ions exist in the ZnO crystal lattices with +1 valence state as discussed in XPS spectra. With increasing the Cu doping concentration, more oxygen vacancies will be introduced in the samples, which finally results in an enhanced green emission in $Zn_{0.97-x}Cu_xCr_{0.03}O$ powders [41].

3.4. Magnetic properties

Fig. 6 shows the dependence of magnetic field (H) on the magnetization (M) at 300 K for pure ZnO and $Zn_{0.97-x}Cu_xCr_{0.03}O$ powders with different Cu concentrations. From Fig. 6 we find that pure ZnO has no magnetic property and the powders of $Zn_{0.97-x}Cu_xCr_{0.03}O$ exhibit ferromagnetism at 300 K. Moreover, after Cu doping into ZnCrO, the magnetization of $Zn_{0.97-x}Cu_xCr_{0.03}O$ increased significantly. With Cu concentration increasing from 0 to 0.02, the remnant magnetization (M_r) increases from 0.0004 to 0.0024 emu/g and the saturation magnetization (M_s) increases from 0.0056 to 0.0088 emu/g.

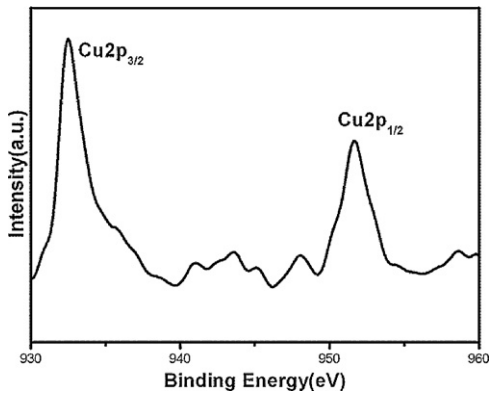

Fig. 4. The Cu 2p core-level photoemission spectra for $Zn_{0.95}Cu_{0.0}Cr_{0.032}O$ samples at room temperature.

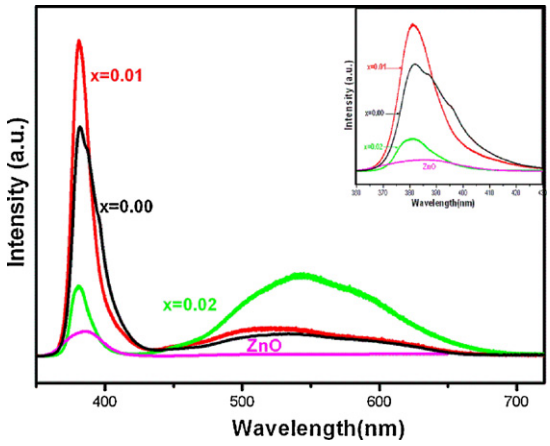

Fig. 5. PL spectra of pure ZnO and $Zn_{0.97-x}Cu_xCr_{0.03}O$ ($x = 0$, 0.01, 0.02) samples.

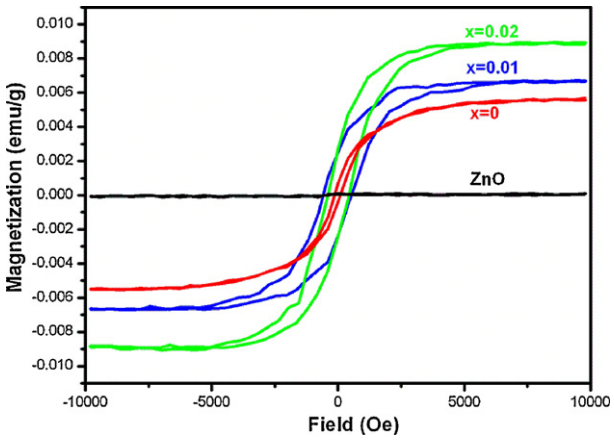

Fig. 6. Magnetic field dependence of magnetization for pure ZnO and $Zn_{0.97-x}Cu_xCr_{0.03}O$ ($x = 0$, 0.01, 0.02, 0.03) samples.

Exchange interaction between Cr 3d and O 2p spin moments should be the main reason for the ferromagnetism behavior in Cr-doped ZnO samples [26]. From the PL data of pure ZnO and ZnCrO, Cr^{3+} incorporation may prompt the formation of Vo, which may be another reason for ZnCrO with weak ferromagnetism. In Cr, Cu co-doped ZnO samples, no trace of CrO_2, which exhibits room-temperature ferromagnetism, can be found in either XRD or XPS measurements when the concentration of Cu is less than 0.02. It can be concluded that the ferromagnetism has nothing to do with the existence of the second phase. Furthermore, the magnetization of $Zn_{0.97-x}Cu_xCr_{0.03}O$ ($x \leq 2$) increases markedly in comparison with that of $Zn_{0.97}Cr_{0.03}O$ samples, which is consistent with the results reported by Lu et al. [4] and Dinesha et al. [17]. In other words, the introduction of the Cu element is conducive to the formation of ferromagnetic order. One reason is attributed to oxygen vacancies (Vo), since in PL spectra we deduce that the Vo density increases with increasing Cu doping concentration. At the Fermi level, Vo can initiate defect-related hybridization and establish a long-rang ferromagnetic ordering [42–44]. The other reason is that the Cu ion with +1 valence state plays the role of the acceptors. Once the Cu ions further substitute the Zn ions, the local hole concentration at the anion site increases, the local density of states (DOS) at the Fermi level increases and the exchange interaction is enhanced [23]. Therefore, the magnetization can be achieved with a reasonable amount of global acceptor concentration. Therefore, the origin of the ferromagnetism in the $Zn_{0.97-x}Cu_xCr_{0.03}O$ ($x \leq 2$) is the Cu and Cr doping, i.e. the room-temperature ferromagnetism of $Zn_{0.97-x}Cu_xCr_{0.03}O$ ($x \leq 2$) was the intrinsic property.

4. Conclusions

In summary, $Zn_{0.97-x}Cu_xCr_{0.03}O$ ($x = 0$, 0.01, 0.02, and 0.03) samples were synthesized by the sol–gel method. The structural, optical and the magnetization properties were investigated. It can be concluded that $Zn_{0.97-x}Cu_xCr_{0.03}O$ samples have wurtzite structure of ZnO with Cu doping concentration increasing up to 2 at%. Compared with the PL spectra of ZnO and ZnCrO, the UV emission of $Zn_{0.97-x}Cu_xCr_{0.03}O$ samples exhibits a blue shift and the intensity of green emission obviously is enhanced due to more oxygen vacancies introduced to the samples. Since the density of oxygen vacancies increases and Cu^{1+} plays the role of the acceptor with Cu doping into the ZnCrO, $Zn_{0.97-x}Cu_xCr_{0.03}O$ samples exhibit ferromagnetism in room-temperature and the saturated magnetization (M_s) increase with Cu doping concentration increasing from 0 to 0.02.

Acknowledgements

This work was supported by the financial support of the National Nature Science Foundation of China (Grant Nos. 10804036; 60778040; 60878039), National Programs for High Technology Research and Development of China (863) (Item No. 2009AA03Z303), the Science and Technology program of Jilin province (No.20080514), and the Open Project Program of National Laboratory of Superhard Materials (No. 201004).

References

[1] X.L. Chen, Z.W. Zhou, K. Wang, X.M. Fan, S.C. Hu, Y. Wang, Y. Huang, Mater. Res. Bull. 44 (2009) 799.
[2] T. Dietl, H. Ohno, F. Matsukura, J. Cibert, D. Ferrand, Science 287 (2003) 1019.
[3] K. Sato, H. Katayama-Yoshida, Physica E 10 (2001) 251.
[4] Z.L. Lu, W. Miao, W.Q. Zou, M.X. Xu, F.M. Zhang, J. Alloys Compd. 494 (2010) 392.
[5] X.J. Liu, X.Y. Zhu, J.T. Luo, F. Zeng, F. Pan, J. Alloys Compd. 482 (2009) 224.
[6] M. Gao, J. Liu, H. Sun, X. Wu, D. Xue, J. Alloys Compd. 500 (2) (2010) 181.
[7] R.K. Singhal, A. Samariya, Y.T. Xing, S. Kumar, S.N. Dolia, U.P. Deshpande, T. Shripathi, E.B. Saitovitch, J. Alloys Compd. 496 (2010) 324.
[8] B. Wang, L.D. Tang, J.Q. Qi, H.L. Du, Z.B. Zhang, J. Alloys Compd. 503 (2010) 436.
[9] C.E. Benouis, M. Benhaliliba, A. Sanchez Juarez, M.S. Aida, F. Chami, F. Yakuphanoglu, J. Alloys Compd. 490 (2010) 62.
[10] R. Wen, L. Wang, X. Wang, G.H. Yue, Y. Chen, D.L. Peng, J. Alloys Compd. 508 (2010) 370.
[11] J.J. Gu, L.H. Liu, H.T. Li, Q. Xu, H.Y. Sun, J. Alloys Compd. 508 (2010) 516.
[12] M. Benhaliliba, C.E. Benouis, M.S. Aida, A. Sanchez Juarez, F. Yakuphanoglu, A. Tiburcio Silver, J. Alloys Compd. 506 (2010) 548.
[13] Y.X. Liu, H.L. Zhang, X.Y. An, C.T. Gao, Z.X. Zhang, J.Y. Zhou, M. Zhou, E.Q. Xie, J. Alloys Compd. 506 (2010) 772.
[14] T. Prasada Rao, M.C. Santhosh Kumar, J. Alloys Compd. 506 (2010) 788.
[15] Q. Xu, L. Hartmann, H. Schmidt, H. Hochmuth, M. Lorenz, A. Setzer, P. Esquinazi, C. Meinecke, M. Grundmann, Thin Solid Films 516 (2008) 1160.
[16] G.R. Li, D.L. Qu, W.X. Zhao, Y.X. Tong, Electrochem. Commun. 9 (2007) 1661.
[17] M.L. Dinesha, H.S. Jayanna, S. Mohanty, S. Ravi, J. Alloys Compd. 490 (2010) 618.
[18] N. Brihi, A. Bouaine, A. Berbadj, G. Schmerber, S. Colis, A. Dinia, Thin Solid Films 518 (2010) 4549.
[19] D. Chakraborti, S. Ramachandran, G. Trichy, J. Narayan, J. Appl. Phys. 101 (2007) 053918.
[20] H.T. Lin, T.S. Chin, J.C. Shih, S.H. Lin, T.M. Hong, Appl. Phys. Lett. 85 (2004) 621.
[21] N. Brihi, S.T. Hussain, M. Usman, S.K. Hasanain, A. Mumtaz, Appl. Surf. Sci. 255 (2009) 8506.
[22] J. Qi, D.Q. Gao, L. Zhang, Y.H. Yang, Appl. Surf. Sci. 256 (2010) 2507.
[23] Y.Y. Wei, D.L. Hou, S. Qiao, C.M. Zhen, G.D. Tang, Physica B 404 (2009) 486.
[24] J.M.D. Coey, M. Venkatesan, C.B. Fitzgerald, Nat. Mater. 4 (2005) 173.
[25] M. Venkatesan, C.B. Fitzgerald, J.G. Lunney, J.M.D. Coey, Phys. Rev. Lett. 93 (2004) 17720.
[26] Y. Liu, J.H. Yang, Q.F. Guan, L.L. Yang, Y.J. Zhang, Y.X. Wang Feng, J. Cao, X.Y. Liu, Y.T. Yang, M.B. Wei, J. Alloys Compd. 486 (2009) 835.
[27] H.L. Liu, J.H. Yang, Y.J. Zhang, Y.X. Wang, M.B. Wei, D.D. Wang, L.Y. Zhao, J.H. Lang, M. Gao, J. Mater. Sci.: Mater. Electron. 20 (2009) 628.
[28] M Wei, N. Braddon, D. Zhi, P.A. Midgley, S.K. Chen, M.G. Blamire, J.L. MacManus-Driscoll, Appl. Phys. Lett. 86 (2005) 72514.
[29] J.H. Yang, L.Y. Zhao, X. Ding, L.L. Yang, Y.J. Zhang, Y.X. Wang, H.L. Liu, Mater. Sci. Eng., B 162 (2009) 143.
[30] F. Yakuphanoglu, J. Alloys Compd. 507 (2010) 184.
[31] Y.B. Li, Y. Li, M.Y. Zhu, T. Yang, J. Huang, H.M. Jin, Y.M. Hu, Solid State Commun. 150 (2010) 751.
[32] B.Q. Wang, J. Iqbal, X.D. Shan, G.W. Huang, H.G. Fu, R.H. Yu, D.P. Yu, Mater. Chem. Phys. 113 (2009) 103.
[33] Z. Jin, T. Fukumura, M. Kawasaki, K. Ando, H. Saito, T. Sekiguchi, Y.Z. Yoo, M. Murakami, Y. Matsumoto, T. Hasegawa, H. Koinuma, Appl. Phys. Lett. 78 (2001) 3824.
[34] C.K. Xu, K.K. Yang, Y.Y. Liu, L.W. Huang, H. Lee, J. Cho, H. Wang, J. Phys. Chem. C 112 (2008) 19236.
[35] J.H. Yang, M. Gao, Y.J. Zhang, L.L. Yang, J.H. Lang, D.D. Wang, Y.X. Wang, H.L. Liu, H.G. Fan, M.B. Wei, F.Z. Liu, Chem. Res. Chin. Univ. 24 (2008) 1005.
[36] Y. Liu, J.H. Yang, Q.F. Guan, L.L. Yang, H.L. Liu, Y.J. Zhang, Y.X. Wang, D.D. Wang, J.H. Lang, Y.T. Yang, L.H. Fei, M.B. Wei, Appl. Surf. Sci. 256 (2010) 3559.
[37] P. Zu, Z.K. Tang, G.K.L. Wong, M. Kawasaki, A. Ohtomo, H. Koinuma, Y. Segawa, Solid State Commun. 103 (1997) 459.
[38] D.M. Bagnall, Y.F. Chen, M.Y. Shen, Z. Zhu, T. Goto, T. Yao, J. Cryst. Growth 184 (1998) 605.

[39] L.L. Yang, Q.X. Zhao, M. Willander, J.H. Yang, I. Ivanov, J. Appl. Phys. 105 (2009) 053503.
[40] W. Li, D. Mao, F. Zhang, X. Wang, X. Liu, S. Zou, Y. Zhu, Q. Li, J. Xu, Nucl. Instrum. Methods: Phys. Res. B 169 (2000) 59.
[41] K. Samanta, P. Bhattacharya, R.S. Katiyarl, J. Alloys Compd. 105 (2009) 113929.
[42] G.Z. Xing, D.D. Wang, J.B. Yi, L.L. Yang, M. Gao, M. He, J.Y. Yang, J. Ding, T.C. Sum, T. Wu, Appl. Phys. Lett. 96 (2010) 112511.
[43] G.Z. Xing, J.B. Yi, D.D. Wang, L. Liao, T. Yu, Z.X. Shen, C.H.A. Huan, T.C. Sum, J. Ding, T. Wu, Phys. Rev. B 79 (2009) 174406.
[44] Y.F. Li, R. Deng, B. Yao, G.Z. Xing, D.D. Wang, Tom Wu, Appl. Phys. Lett. 97 (2010) 102506.